

THE DIFFERENTIAL CROSS SECTION FOR ELECTRON
CAPTURE FROM HELIUM BY 293 keV PROTONS

by

Tom R. Bratton

B. S., Nebraska Wesleyan University, 1975

A MASTER'S THESIS
submitted in partial fulfillment of the
requirements for the degree
MASTER OF SCIENCE

Department of Physics
KANSAS STATE UNIVERSITY
Manhattan, Kansas 66506

1977

C. K. Cochrane
Major Professor

LD
2668
T4
1977
B73
C-2
Document

115

TABLE OF CONTENTS

	Page
LIST OF FIGURES	1
ACKNOWLEDGEMENTS	11
I. Introduction	1
II. Experimental Apparatus	6
III. Experimental Results and Methods	12
A. Gas Pressure Dependence Curves	
B. Differential Cross Section for Protons on Helium	
C. Angular Resolution	
D. Differential Cross Section for Protons on Nitrogen	
E. Energy Calibration	
IV. Conclusions	42
REFERENCES	44
APPENDIX	45
ABSTRACT	48

LIST OF FIGURES

- Fig. 1 Potential diagram.
- Fig. 2 Schematic of experimental apparatus, not to scale.
- Fig. 3 Electronics.
- Fig. 4 Gas pressure dependence for protons on helium at 293 keV.
- Fig. 5 Gas pressure dependence for protons on helium at 1000 keV.
- Fig. 6 Differential cross section for elastic scattering of protons on helium at 293 keV.
- Fig. 7 Differential cross section for capture of electrons from helium by 293 keV protons.
- Fig. 8 Overlay of the Born (C) calculation on the experimental results of protons on helium.
- Fig. 9 θ^* verses energy.
- Fig. 10 Experimental Resolution.
- Fig. 11 Convolution of Born (C).
- Fig. 12 Convolution of Band FOPT.
- Fig. 13 Differential cross section for capture of electrons from nitrogen by 293 keV protons.
- Fig. 14 Yield of gamma rays verses hall probe voltage for accelerator energy calibration.

ACKNOWLEDGEMENTS

I wish to dedicate this work to my parents, Elvin and Lena Bratton, for their guidance, encouragement, and support.

I would like to thank Lew Cocke for his help through the course of this work. His patience, encouragement, and helpful discussions were greatly appreciated.

I would to thank Basil Curnutte, Larry Weaver, and Jim Macdonald for their helpful comments and Jim McGuire and Yedula Band for their unpublished calculations.

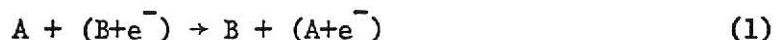
I wish to acknowledge Jim Guffey for making the neutral detector collimator used in this experiment and Clarence Annett for helping take the data.

I wish to thank all my friends and especially Bill Paske and Sheila Gunn for helping me make it through Graduate School.

I also wish to acknowledge the financial support of the Agricultural Experiment Station.

I. Introduction

Electron capture is the transfer of a single active electron from one nucleus to another during a collision.



In this experiment, the reaction

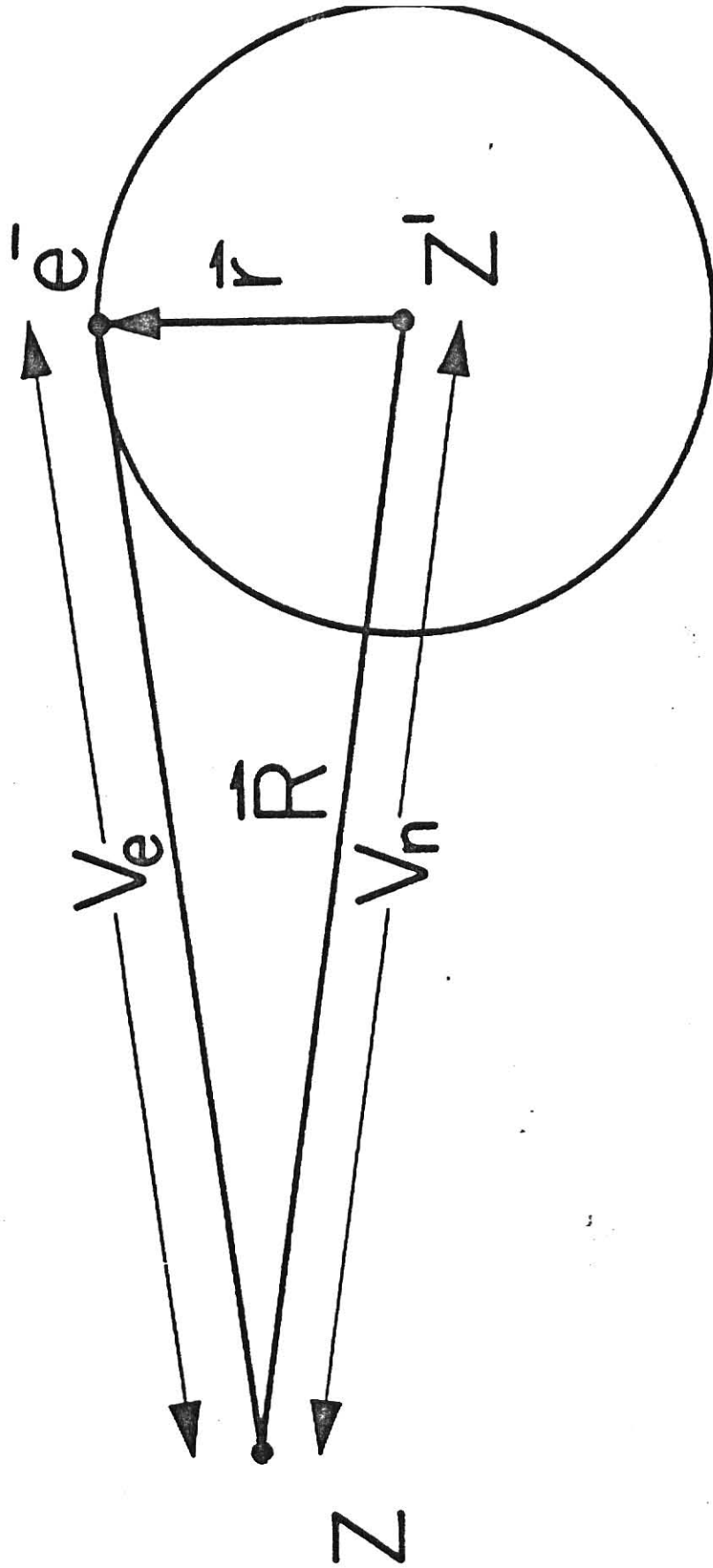


was studied for projectile velocities comparable to or exceeding the orbital velocity of the active target electron. Protons, incident on helium gas, captured an electron and scattered as neutral hydrogen atoms.

Much theoretical study¹ has been devoted to the problem of electron capture. Historically, the first and easiest calculation was due to Oppenheimer,² and Brinkman and Kramers.³ The calculation of the scattering amplitude was computed in first order perturbation theory using only $V_e = -Ze^2/|\vec{R}-\vec{r}|$, the interaction between the projectile and the electron (see Figure 1). What was gained in ease of calculation was sacrificed in accuracy: The total electron capture cross section for protons on helium, was calculated to be several times larger than the experimental cross section.

Other calculations,⁴⁻⁶ which included the nuclear interaction, $V_n = \frac{ZZ'e^2}{|\vec{R}|}$, were slightly more successful. Jackson and Schiff⁴ used the complete interaction Hamiltonian, $V_e + V_n$, for calculating the total charge exchange cross section for protons on hydrogen, and found good

Figure 1: Diagram showing the coordinates of the particles
and the potentials between them.



agreement between theory and experiment for all energies greater than 25 keV.

Further calculations using the complete interaction Hamiltonian on heavier systems were not nearly as good. Halpern and Law⁵ calculated the k-shell electron capture cross sections for a number of heavy-ion collisions and found them to be very much larger than experiment.

Omidvar, et al.,⁶ found fair agreement to the k-shell electron capture cross section for protons on argon by dropping the target Z dependence in the internuclear interaction. This was necessary in order that the total projectile-target interaction go to zero at large distances.

Objections to the inclusion of the nuclear term arose on the physical grounds that the mutual repulsion of the nuclei should not directly influence the electronic transition probability. A solution to this problem was given by Bates.⁷ In deriving the correct expression for the scattering amplitude given by first order perturbation theory for systems with non-orthogonal unperturbed initial and final states, it was seen that the nuclear interaction term should be replaced by another term similar in effect but different in origin. The correct expression for the transition matrix is

$$\frac{\langle f | V_e - \langle i | V_e | i \rangle | i \rangle}{1 - |\langle f | i \rangle|^2} \quad (3)$$

where V_e is the interaction between the projectile with coordinate \vec{R} and the electron with coordinate \vec{r} , $|i\rangle$ is the initial state with the electron bound to Z' , and $\langle f|$ is the final state with the electron bound to Z .

Electron capture cross sections to excited states using this form of the Born Approximation have been evaluated by Winter and Lin⁸ for protons on helium. However, neither capture cross sections to the ground state nor differential cross sections were evaluated.

Several different approximations to the transition matrix have been calculated. The approximation $\langle i | V_e | i \rangle = -Ze^2/|\vec{R}|$, equivalent to Omidvar's⁶ Born (C) calculation, was used in calculating the total and differential cross sections for electron capture from several gases by protons. This calculation gave satisfactory agreement to total electron capture cross sections for protons on argon⁶ and helium⁹ but predicted a zero in the differential cross sections.

Cocke, et al.,¹⁰ measured the differential cross section for electron capture from argon by 6 MeV protons. The differential cross section was found to decrease monotonically with scattering angle showing no indication of a zero. It was pointed out, however, that the presence of outer shell electrons might substantially modify the calculated angular distribution, since the Born (C) calculation only considered capture of an electron from an isolated hydrogenic k-shell. The measurement of the differential cross section for the capture of electrons from helium by protons would thus be of interest since no effect could be attributed to outer shell electrons.

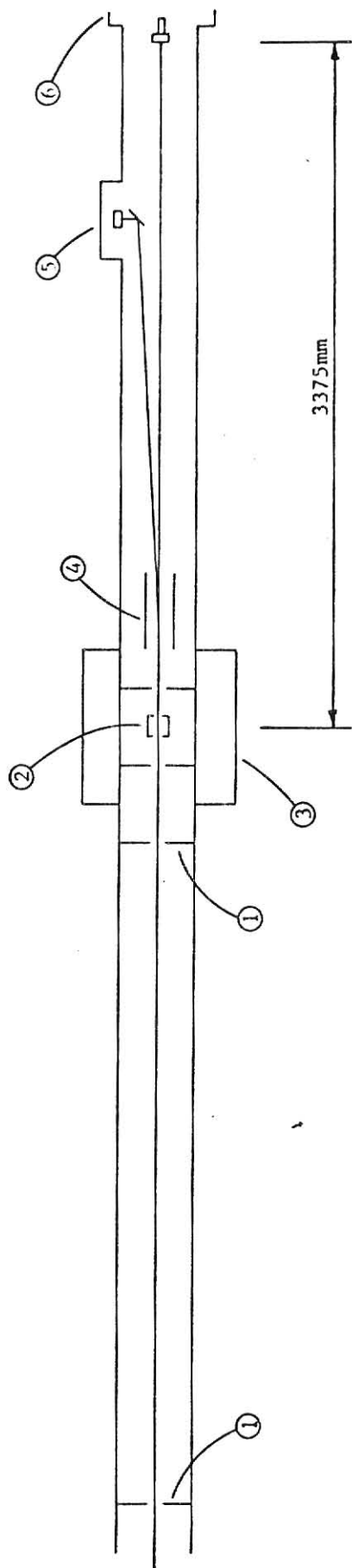
II. Experimental Apparatus

The purpose of this experiment was to measure the differential cross section for electron capture from helium by protons. Since several calculations^{6,9,11} predicted a node in the differential cross section, the experiment was designed so that the measurements would resolve this structure. This chapter will discuss the apparatus used in this experiment.

A beam of 293 keV protons was produced by Kansas State University's 3 MV Van de Graaff Accelerator. The beam passed through a switching magnet which deflected the protons of the appropriate energy into our beamline. Figure 2 shows a schematic of our experimental arrangement. Two sets of adjustable four-jaw slits, separated by 2699 mm, defined a path into the gas cell, which was located 137 mm downstream from the second set of slits. The 15-mm-long gas cell was surrounded by an intermediate-pressure region that extended 50 mm along the beamline and was evacuated by an oil diffusion pump which provided differential pumping. A vacuum of 7.0×10^{-7} Torr was maintained in the beamline while pressures of 20-25 mTorr existed in the gas cell. When helium was used as the target gas, a liquid nitrogen trap was placed on the incoming helium gas to trap any condensible vapor contamination.

Scattered particles proceeded through to a surface barrier detector which was collimated by a rectangular aperture of dimensions .137 x .198 mm. The aperture was constructed by gluing four razor blade edges to a metal holder. The detector, located 3375 mm from the gas cell, could be scanned in both dimensions perpendicular to the beam.

Figure 2: Schematic of experimental apparatus, not to scale.



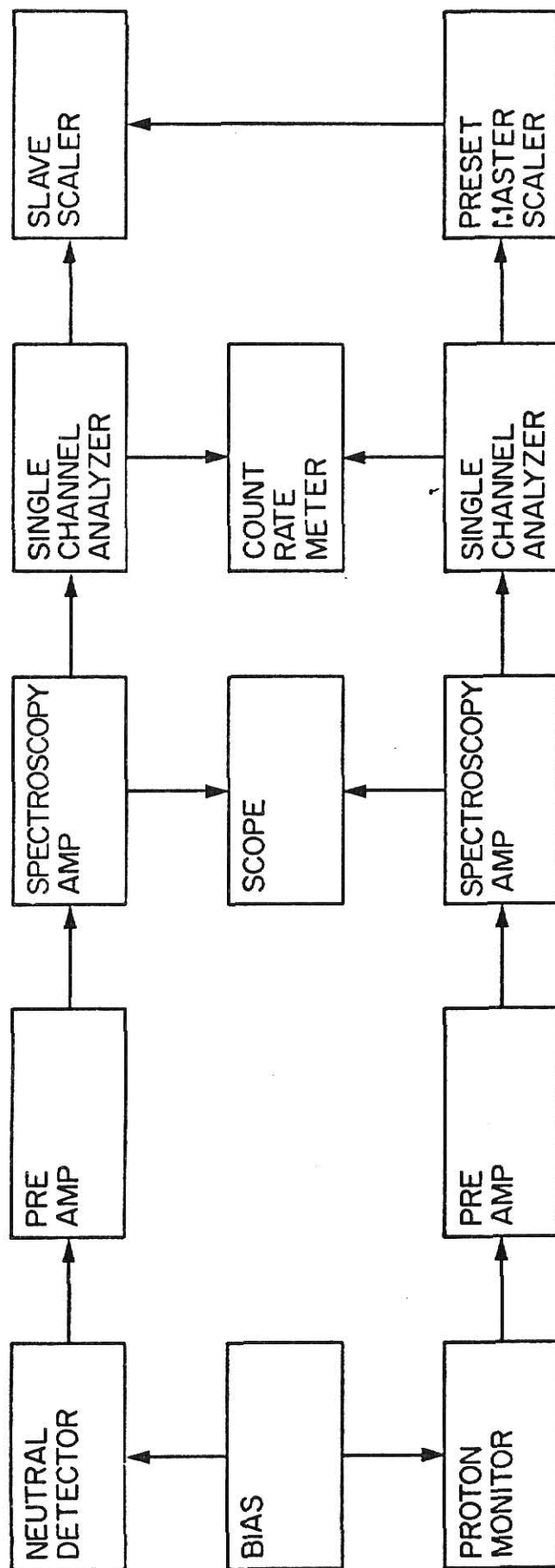
- ① ADJUSTABLE SLITS
- ② GAS CELL
- ③ DIFFUSION PUMP
- ④ ELECTROSTATIC DEFLECTOR
- ⑤ PROTON MONITOR
- ⑥ SCANNING SURFACE BARRIER DETECTOR

DIMENSIONS OF APERTURE:
0.137 x 0.198 (mm)

Because beam currents were too small to measure directly, a proton monitor was installed in order to measure a quantity proportional to the number of incident particles. The charged component of the scattered beam could be deflected into the proton monitor with the use of the electrostatic plates located downstream from the gas cell. The monitor used a thick gold foil inclined at 45° to the beam, to scatter particles into a second surface barrier detector. A Faraday cup placed behind the foil prevented protons from reaching the vicinity of the neutral detector. The purpose of the monitor was two-fold. First, it kept protons from reaching the neutral detector and increasing its background counting rate. Second, because the proton beam intensity produced by the accelerator was constant only over short periods of time (not more than 5 minutes), the monitor count rate, which was proportional to the beam intensity, provided a normalization for the neutral detector count rate.

A schematic of the electronics is shown in Figure 3. A voltage supply provided bias for both detectors. The signal from each detector was amplified by a pre-amp before being amplified by a spectroscopy amp whose unipolar outputs could be viewed by an oscilloscope. The bipolar outputs were sent to a single channel analyzer where discriminators could be set to select the desired pulse height. The lower discriminator was set above the detector noise and the upper discriminator was set just above the pulse. A countrate meter was connected to the output of the monitor single channel analyzer for convenience. The output of each single channel analyzer drove a scaler with the neutral detector scaler being gated by the monitor scaler in such a way that the neutrals scaler counted for a pre-set number of monitor counts.

Figure 3: Electronics



III. Experimental Results and Methods

To ensure that the measurements in this experiment were taken under single-collision conditions, it was necessary to measure the dependence of the yield of neutral particles on gas-cell pressure. Single-collision conditions would imply a linear relationship between the yield of neutrals and the pressure rise in the gas cell for all scattering angles. In measuring the gas pressure dependence, the neutrals were detected by the scanning surface barrier detector and the yield was normalized to the proton monitor. The pressure was measured in the intermediate pressure region by an ionization gauge.

The yield of neutrals was taken to be the difference between the measured yield at each pressure and the yield at base pressure. Figure 4 shows the dependence of the yield of neutrals on pressure rise in the gas cell for two different angles for protons on helium at 293 keV. It is seen that for a pressure rise of 3.15×10^{-6} Torr, illustrated by an arrow in the figure, the yield of neutrals is linear with pressure rise for both angles.

The gas pressure dependence measurement was also made for protons on helium at 1000 keV. The experimental arrangement and procedure was identical to that at 293 keV. As can be seen in figure 5, a pressure rise of 11.5×10^{-6} Torr was acceptable.

The differential cross section is defined by

$$\frac{d\sigma}{d\Omega} = \frac{y}{n_i n_t \Delta\Omega} \quad (4)$$

where y is the number of scattered particles, n_i is the number of incident

Figure 4: Gas pressure dependence for protons on helium
at 293 keV.

**THIS BOOK
CONTAINS
NUMEROUS
PAGES THAT ARE
CUT OFF**

**THIS IS AS
RECEIVED FROM
THE CUSTOMER**

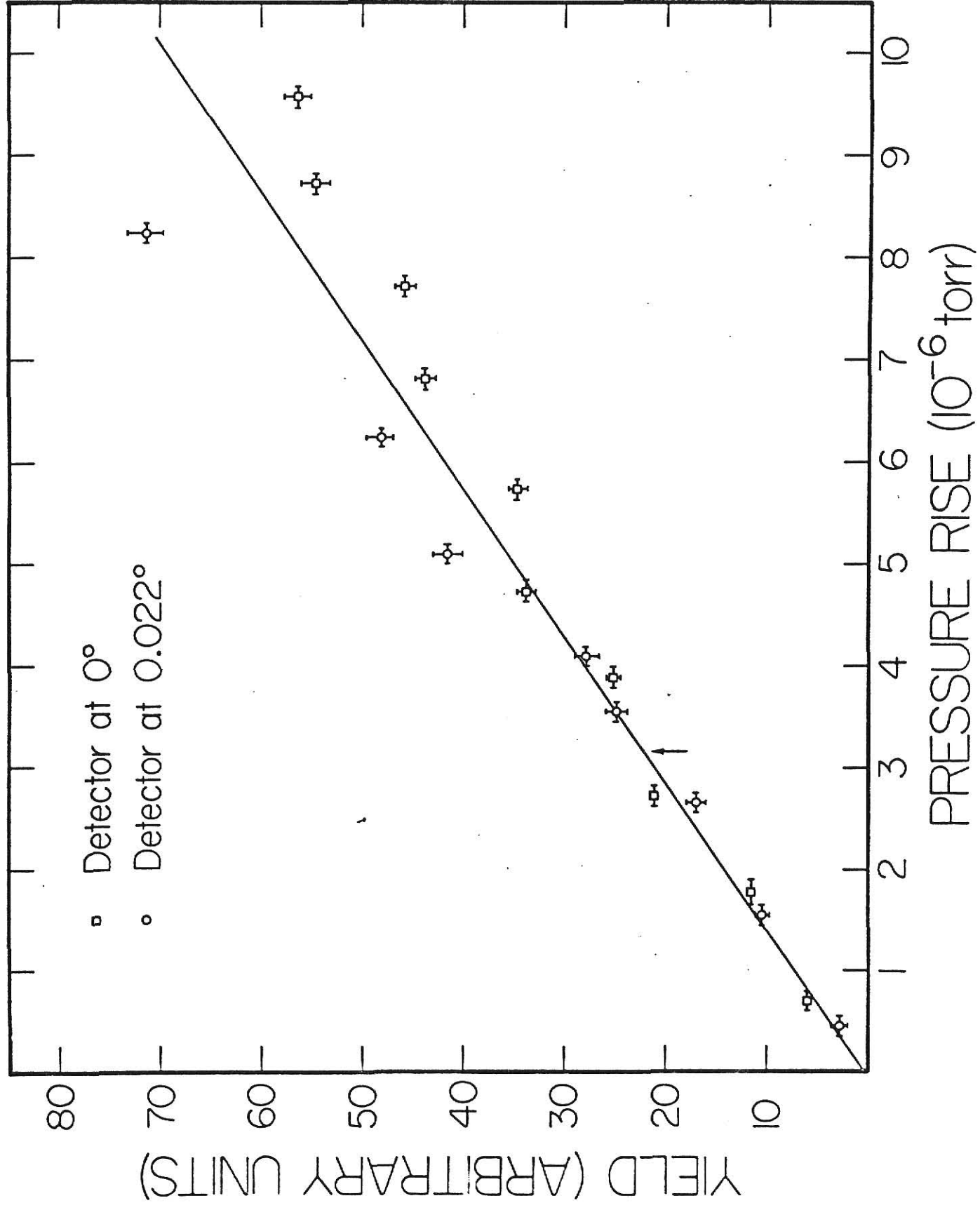
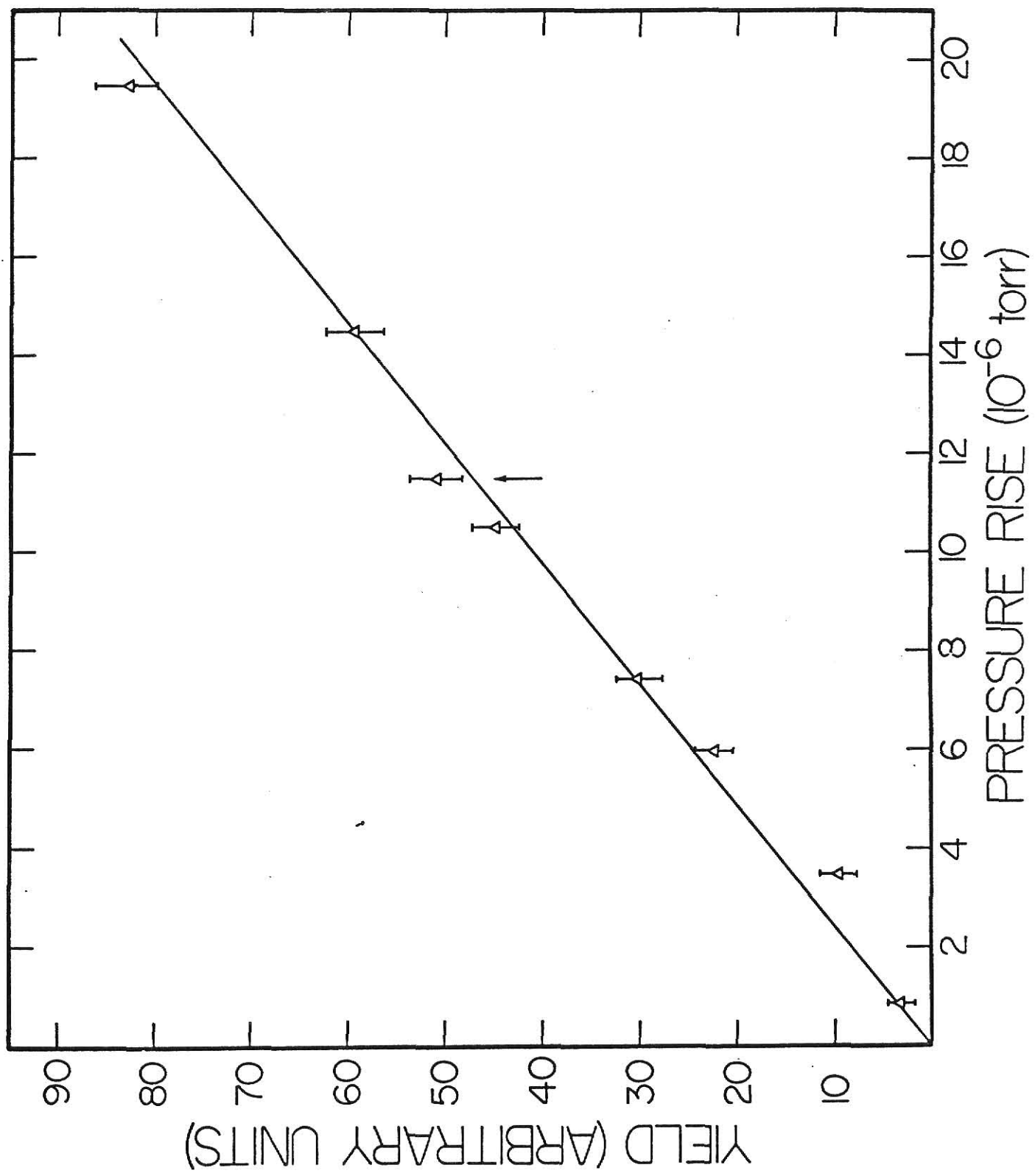


Figure 5: Gas pressure dependence for protons on helium
at 1000 keV.



particles, n_t is the number of scattering centers per square centimeter, and $\Delta\Omega$ is the solid angle subtended by the detector. Since the number of incident particles, n_i , is proportional to the number of monitor counts, n_m ,

$$n_i = C n_m \quad (5)$$

we can rewrite the differential cross section as

$$\frac{d\sigma}{d\Omega} = \left(\frac{y}{n_m} \right) \left(\frac{1}{n_t C \Delta\Omega} \right) \equiv \left(N \right) \left(K \right) . \quad (6)$$

The first term of the product, N , is the yield of particles normalized to the proton monitor. The second term, K , is a constant dependent on the gas cell pressure, the efficiency of the proton monitor, and the solid angle subtended by the detector.

To measure the differential cross section for the capture of electrons, the neutral detector was scanned along the diameter of the hydrogen beam. In order to subtract the neutral background due to residual gas, slit scattering, and other sources, the ratio of neutrals to monitor counts was measured at each angle with gas in and gas out of the cell, before the detector was moved to the next angle. For protons on helium at 293 keV, the neutral count rate was about 140 Hz. at 0° falling to about 1.4 Hz. at $.06^\circ$; the signal to background ratio was about 100 at 0° falling to about 1 at $.06^\circ$. A smooth curve was drawn through the background and subtracted from the yield of neutrals measured with helium in the gas cell. This difference, N , was used in the calculation of the differential cross section.

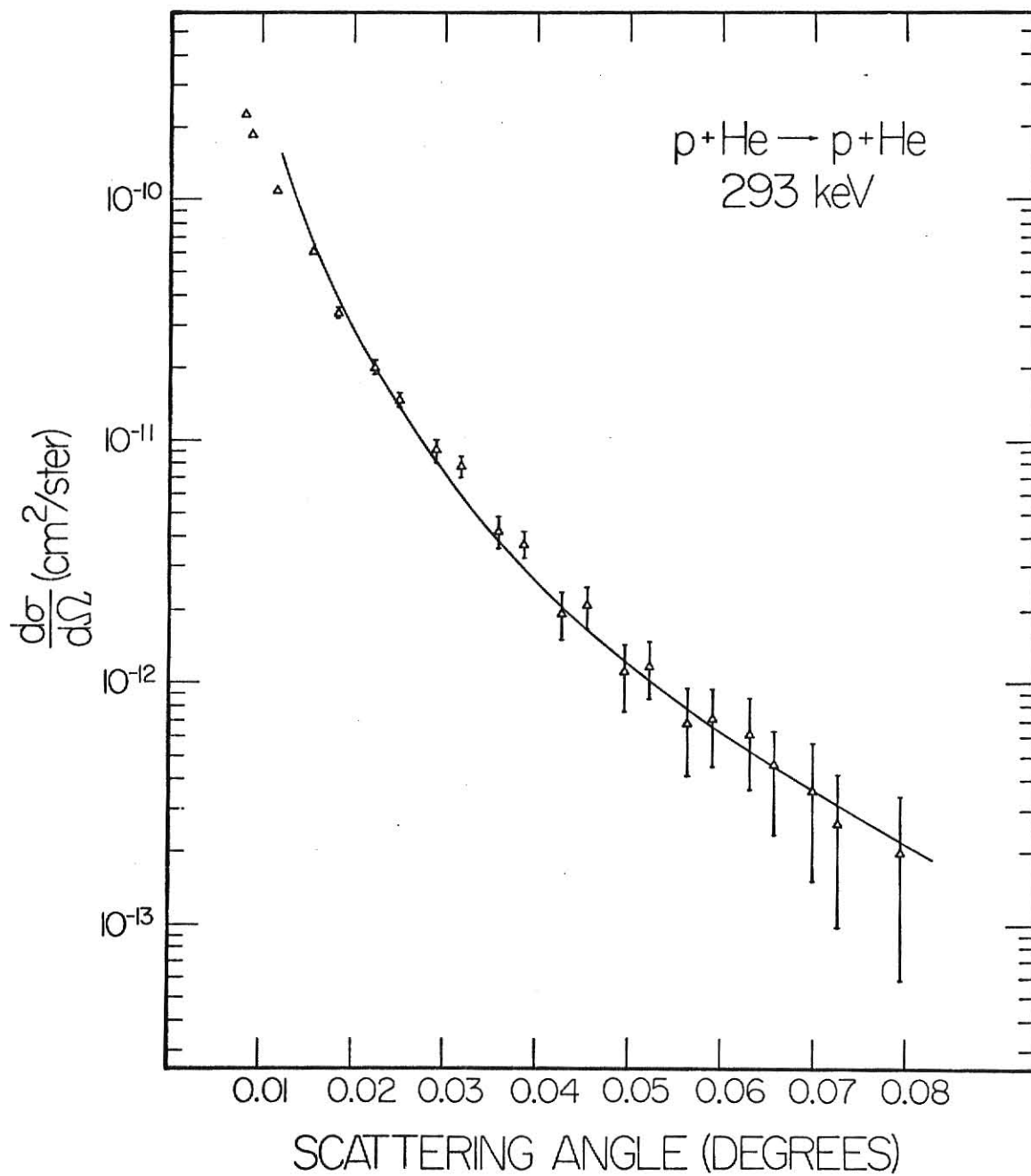
In order to find absolute cross sections, the constant K must be evaluated. This could have been computed directly, by measuring the quantities involved in K, but was measured indirectly by the following method. The elastic scattering of 293 keV protons from helium is approximately Rutherford scattering. Therefore, if this differential cross section can be calculated, and the yield of elastically scattered protons can be measured, then the value of K can be evaluated from the ratio of these two quantities.

To make this measurement the electrostatic plates were grounded so the scattered protons could be detected with the scanning detector. Since the proton monitor was now inoperative, a different normalization procedure was used. The proton beam produced by the accelerator was constant over short periods of time. Therefore, by measuring the yield of protons per time and separately, the number of monitor counts per time, the yield of protons per monitor was calculated.

The pressure of helium in the gas cell was the same for this measurement as in the previous measurement of N. A smooth curve was fit to the background and subtracted from the yield of protons to give N.

The angular distribution for elastic scattering of 293 keV protons from helium was fit to Rutherford scattering modified by a screening parameter.¹⁶ The data and the best curve are plotted in Figure 6. The ratio of the differential cross section for screened Rutherford scattering to Rutherford scattering was found to be .80 at $.07^\circ$ and .68 at $.04^\circ$. The best fit corresponded to a screening radius of $.3295 \text{ \AA}$ but the fit was not sensitive to this parameter. The ratio of the calculated differential cross section for the elastic scattering of protons on helium to the

Figure 6: Differential cross section for the elastic scattering of protons on helium at 293 keV verses proton scattering angle.



measured yield of protons gives the desired constant as $(3.041 \pm .366) \times 10^{-12} \text{ cm}^2/\text{ster.}$

The product of the constant K, and the yield of neutrals is the differential cross section for charge exchange. Figure 7 shows a plot of the differential cross section for the capture of electrons from helium at 293 keV versus the hydrogen atom scattering angle. Measurements were made on both sides of the beam and the corresponding value on each side was averaged. A direct measurement of the angular resolution is plotted in the lower left corner. The integrated total charge exchange cross section was found to be $(9.4 \pm 1.4) \times 10^{-19} \text{ cm}^2$, in good agreement with the value of $(8.0 \pm 1.2) \times 10^{-19} \text{ cm}^2$ found previously by Barnett and Reynolds.¹³ Figure 8 shows the Born (C) calculation superimposed on the experimental differential cross section for electron capture from helium.

A measurement of the differential cross section for protons on helium at higher energies was tried but was hampered by very much smaller total cross sections. Even though a measurement of the wide angle scattering was impossible because of too small count rates, a measurement of θ^* , the half angle at which the differential cross section drops to half-maximum, was possible. The experimental arrangement and procedure was the same as described for protons on helium at 293 keV with one exception. The measurement of the constant K was not necessary since only the shape of the differential cross section was needed.

The count rates at maximum were about 40 Hz at 650 keV and 20 Hz at 1000 keV. Figure 9 shows a plot of θ^* versus energy. Only the last three points, 293 keV, 650 keV, and 1000 keV, were measured in this experiment.

Figure 7: Differential cross section for capture of electrons from helium by 293 keV protons verses hydrogen atom scattering angle. The angular resolution is shown in the lower left corner.

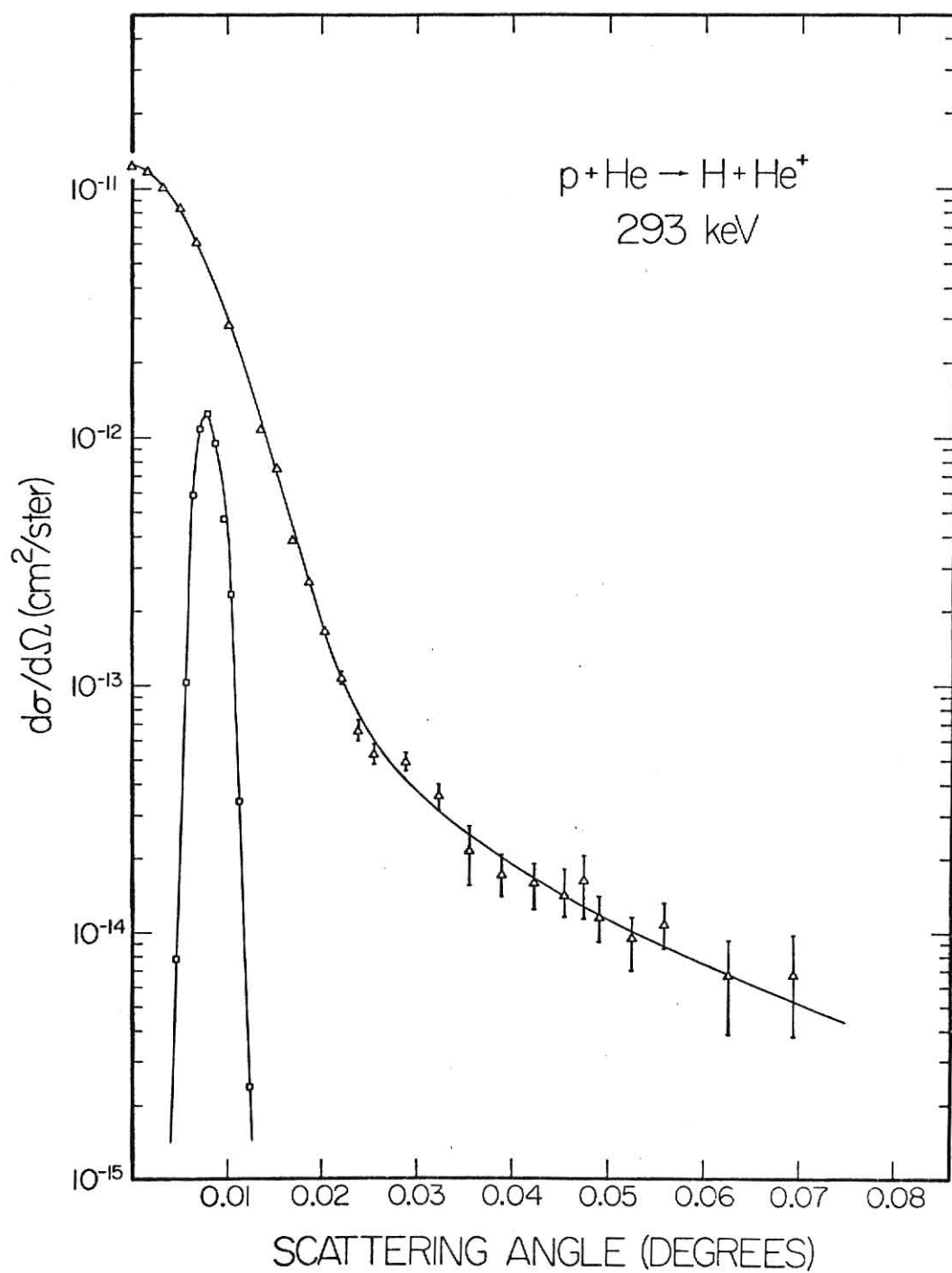


Figure 8: Comparison of the experimental differential cross section with that of the Born (C) calculation. The Born calculation is shown by the dashed line.

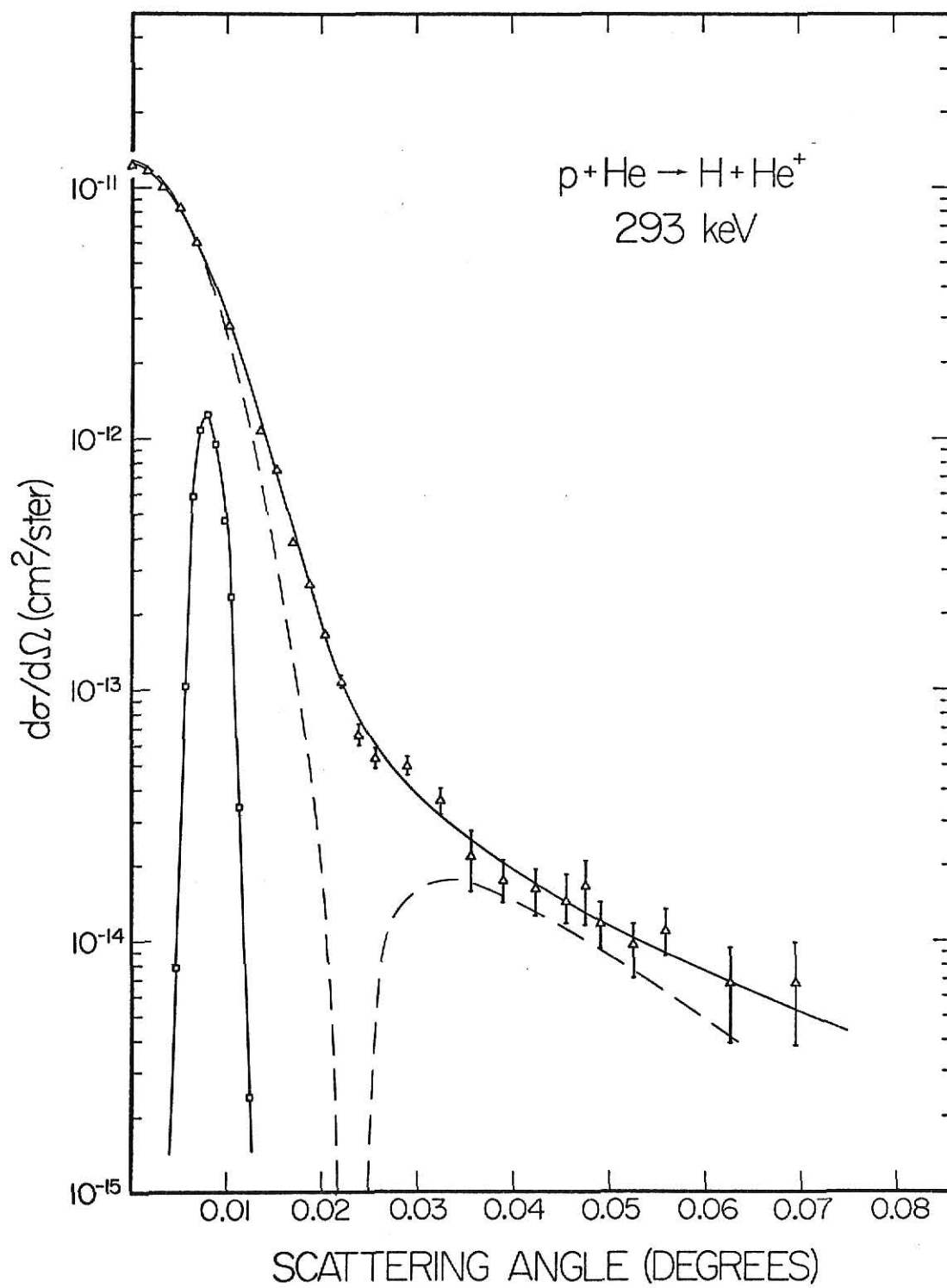
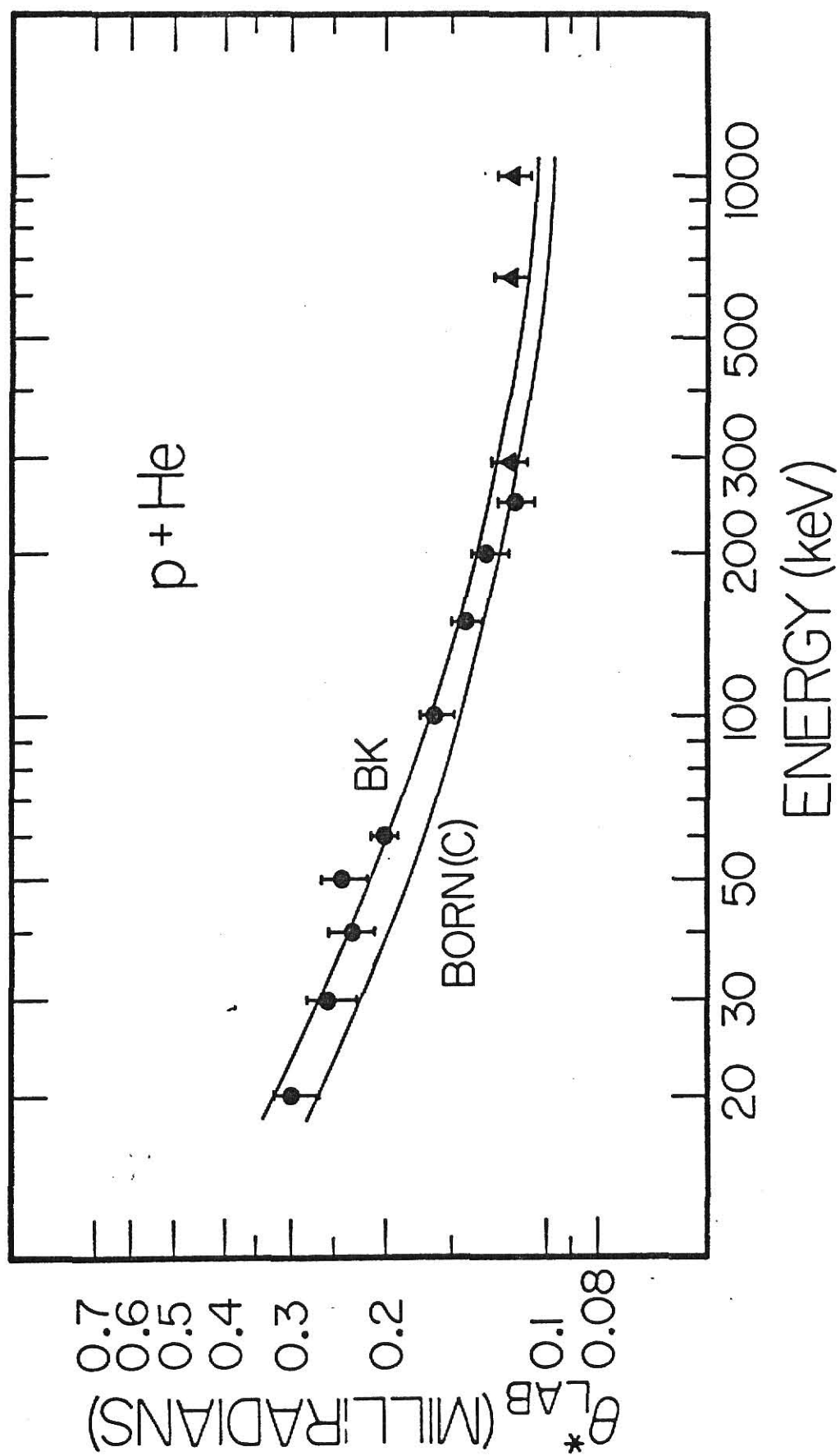


Figure 9: θ^* , half angle at half-maximum, verses proton energy. The circles are from Ref. 12; the triangles are from this thesis.

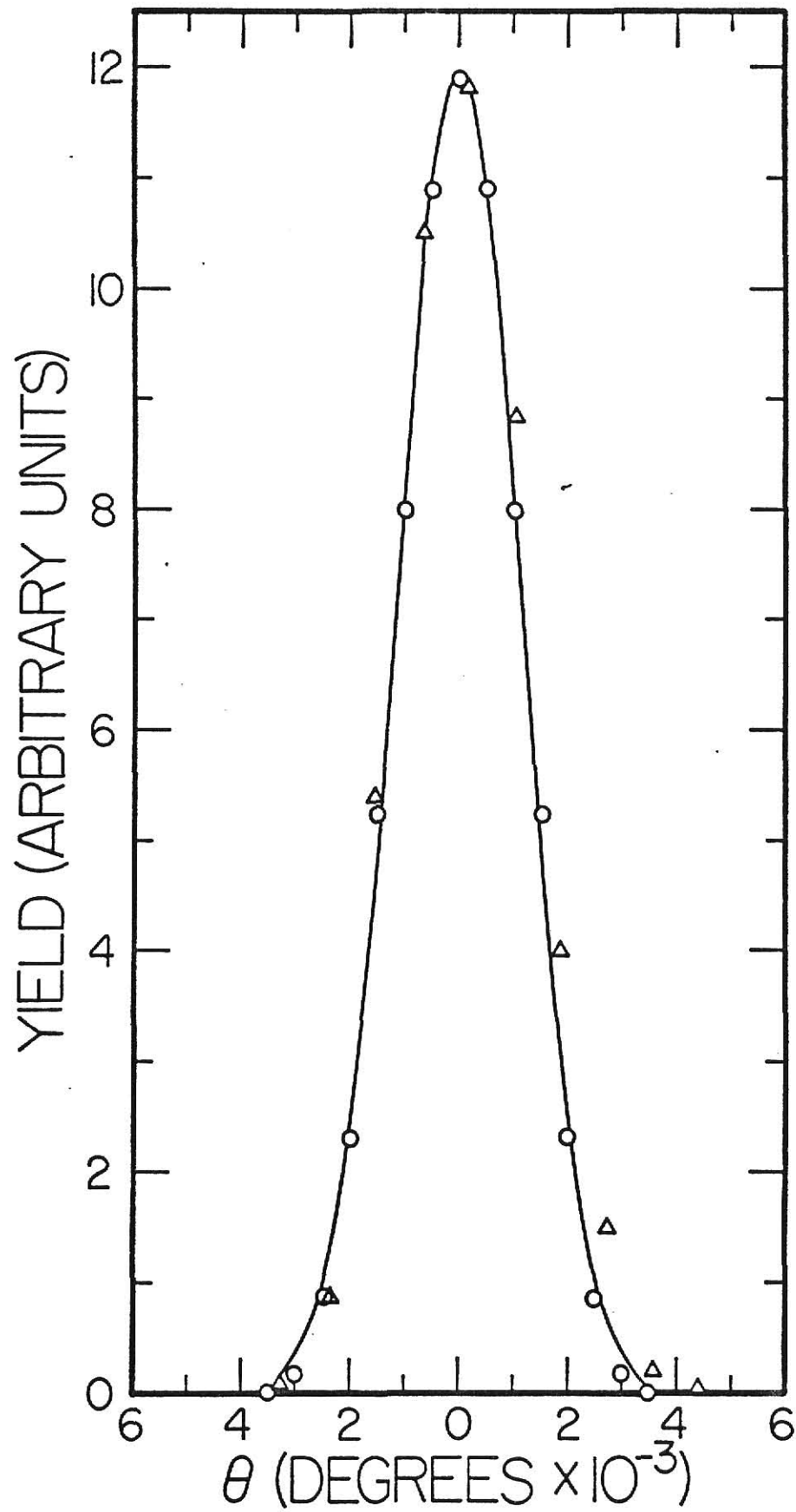


The other data points are due to Wittkower and Gilbody,¹² who had previously measured the differential cross section for electron capture from helium by 60-250 keV protons. However, they did not have the experimental angular resolution needed to see the node in the differential cross section. The upper curve is the Brinkman-Kramers calculation and the lower curve is the Born (C) calculation.

In addition to the measurement of the differential cross section, three auxiliary measurements were carried out. The first was a direct measurement of the angular resolution. The second was a measurement of the differential cross section for the capture of electrons from nitrogen by 293 keV protons. The third was a calibration of the proton beam energy.

A direct measurement of the experimental angular resolution was crucial for resolving fine structure in the differential cross section. This measurement was accomplished by scanning the neutral detector through the center of the proton beam under the same conditions as those used for the measurement of the differential cross section. Since, under these conditions, the very intense direct beam would destroy the detector, a special arrangement was designed to protect it from the direct beam. A thin strip of metal was placed directly over the detector in line-of-sight with the beam. A thin carbon foil was positioned between the metal strip and the detector's collimator in order to scatter a small portion of the proton beam into the open part of the detector. By this method the count rate was reduced to 250 Hz. at the maximum, and the shoulders dropped to less than .3 Hz. Figure 10 shows the experimental angular resolution. The triangles in the figure correspond to

Figure 10: Overall experimental resolution. The triangles refer to experimental data; the circles to a computer simulation.



measured data. The full width at half maximum is calculated to be $.003^\circ$.

A computer program was written to calculate how much of the node in the differential cross section was "washed out" by our finite experimental resolution. The program required as input the position and dimensions of the two sets of four-jaw slits, the position and dimensions of the collimation on the neutral detector, and the theoretical differential cross section as a function of angle. The program calculated from this data a new differential cross section which was the result of the convolution of the theoretical curve and the resolution function. To ensure that the resolution function used by the program, which was calculated from the position and dimensions of all three apertures, was the same resolution as that which was measured, an additional calculation was made. The theoretical differential cross section was replaced by a delta function. If the program correctly calculated the resolution from the position and dimensions of the apertures, the output would be the measured resolution. The result of this calculation are shown as circles in figure 10.

Two theoretical calculations which predicted a node in the differential cross section were convoluted with the resolution function. Figure 11 shows the Born (C) calculation and figure 12 shows Band's¹¹ calculation. It was found that the theoretical differential cross section dropped from three to four orders of magnitude before rising one order of magnitude.

There are several ways in which the node in the differential cross section could be hidden. It is frequently the case that even small contaminations of heavier multi-electron molecules may significantly interfere with

Figure 11: Born (C) calculation.⁶ The solid curve represents the original theoretical curve and the dashed curve represents the result of convoluting the theoretical curve with the experimental resolution.

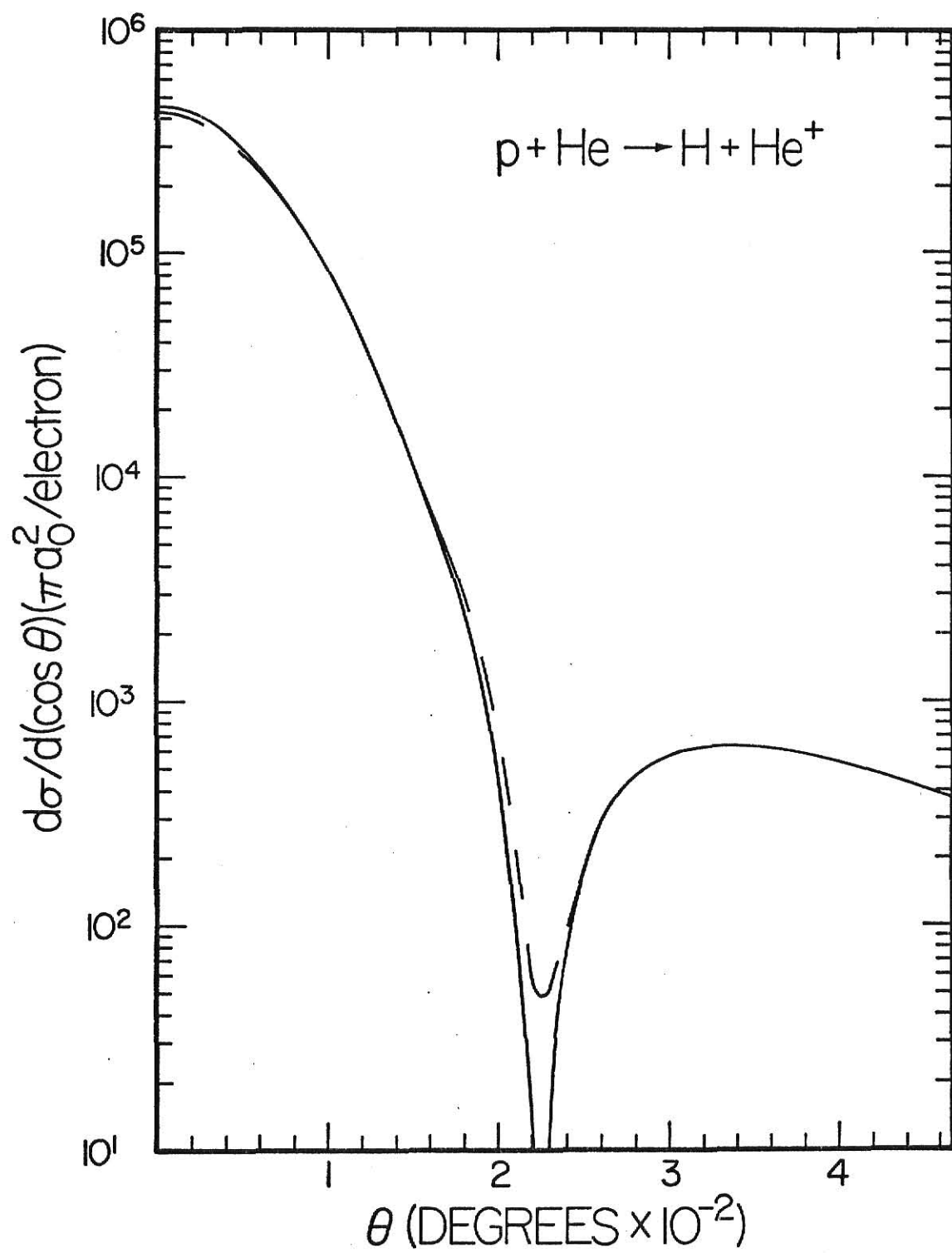
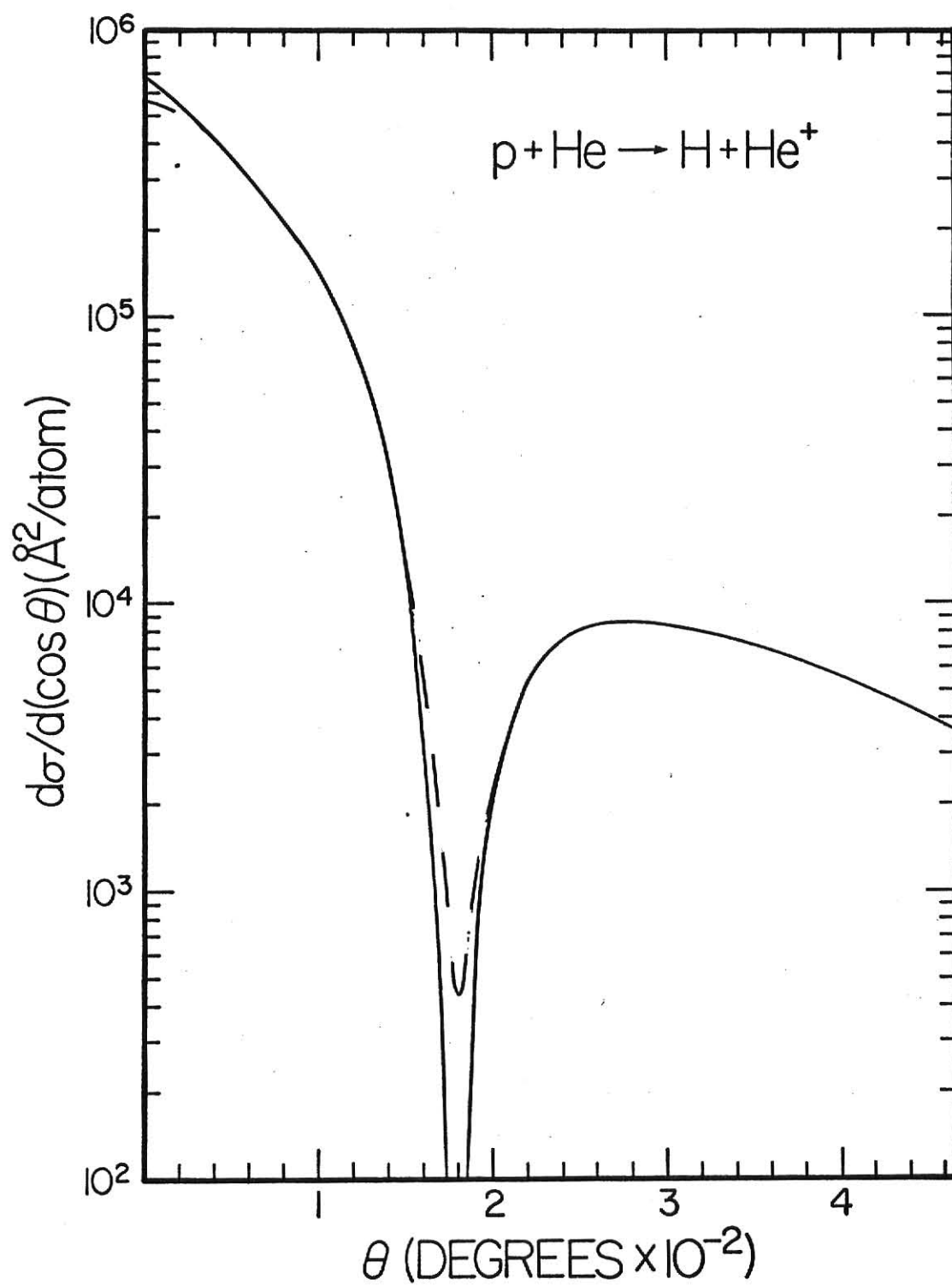


Figure 12: Band's first order perturbation calculation.¹¹

The solid curve represents the original theoretical curve and the dashed curve represents the result of convoluting the theoretical curve with the experimental resolution.



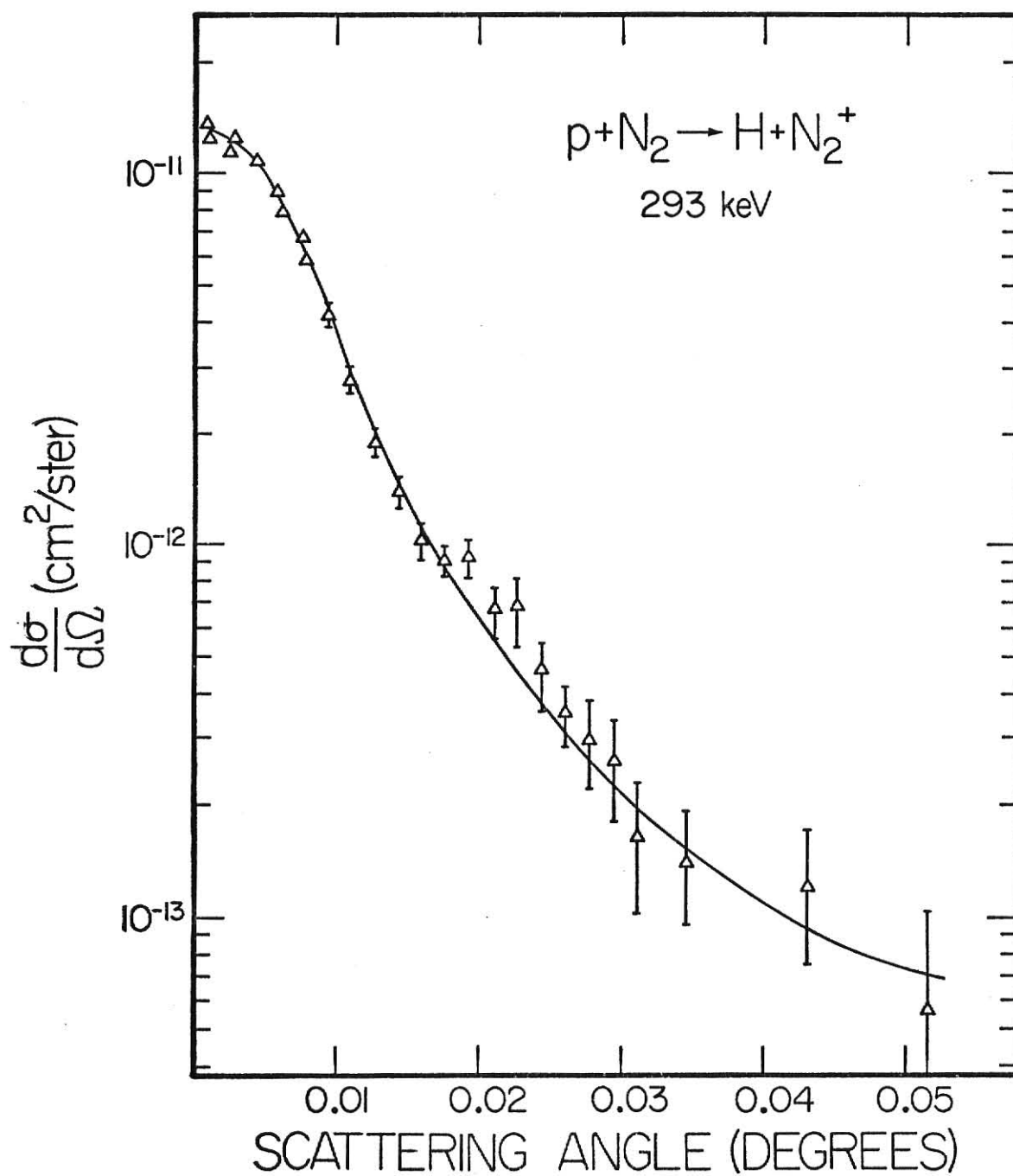
measurements of cross sections on helium targets.

To learn about the effect of contamination the differential cross section for the capture of electrons from nitrogen by 293 keV protons was measured. The experimental method was identical to the protons on helium experiment with the exception that an absolute measurement on the differential cross section was not made. In calculating the differential cross section we integrated the angular distribution and normalized it to the previously measured value of $(1.8 \pm .3) \times 10^{-18} \text{ cm}^2$ by Barnett and Reynolds.¹³ A plot of the differential cross section verses hydrogen atom scattering angle is shown in figure 13.

By comparing the two differential cross sections some conclusions can be drawn about the effects of contamination. Since cross sections are additive, the cross section at any angle is the sum of the cross sections of the gases at that angle times their fractional abundance in the gas cell. Since the total cross section of both gases are nearly equal and the differential cross sections have the same shape for at least one order of magnitude drop in differential cross section, a 20% contamination by the number of atoms of the helium gas with nitrogen would be required to destroy the node.

To determine accurately the energy of the proton beam and calculate a calibration constant for the beamline, the following experiment was completed. The nuclear reaction, $F^{19}(p,\alpha\gamma)O^{16}$, was a nuclear resonance for 340.5 keV protons. Therefore, the experiment consisted of bombarding a thick (1/2 cm) crystal of lithium fluoride with a variable energy proton beam and measuring the increase in yield of the resulting gamma ray. Since the target was a thick target the yield of gamma rays should

Figure 13: The differential cross section per target atom for the capture of electrons from nitrogen gas by 293 keV protons versus hydrogen atom scattering angle.

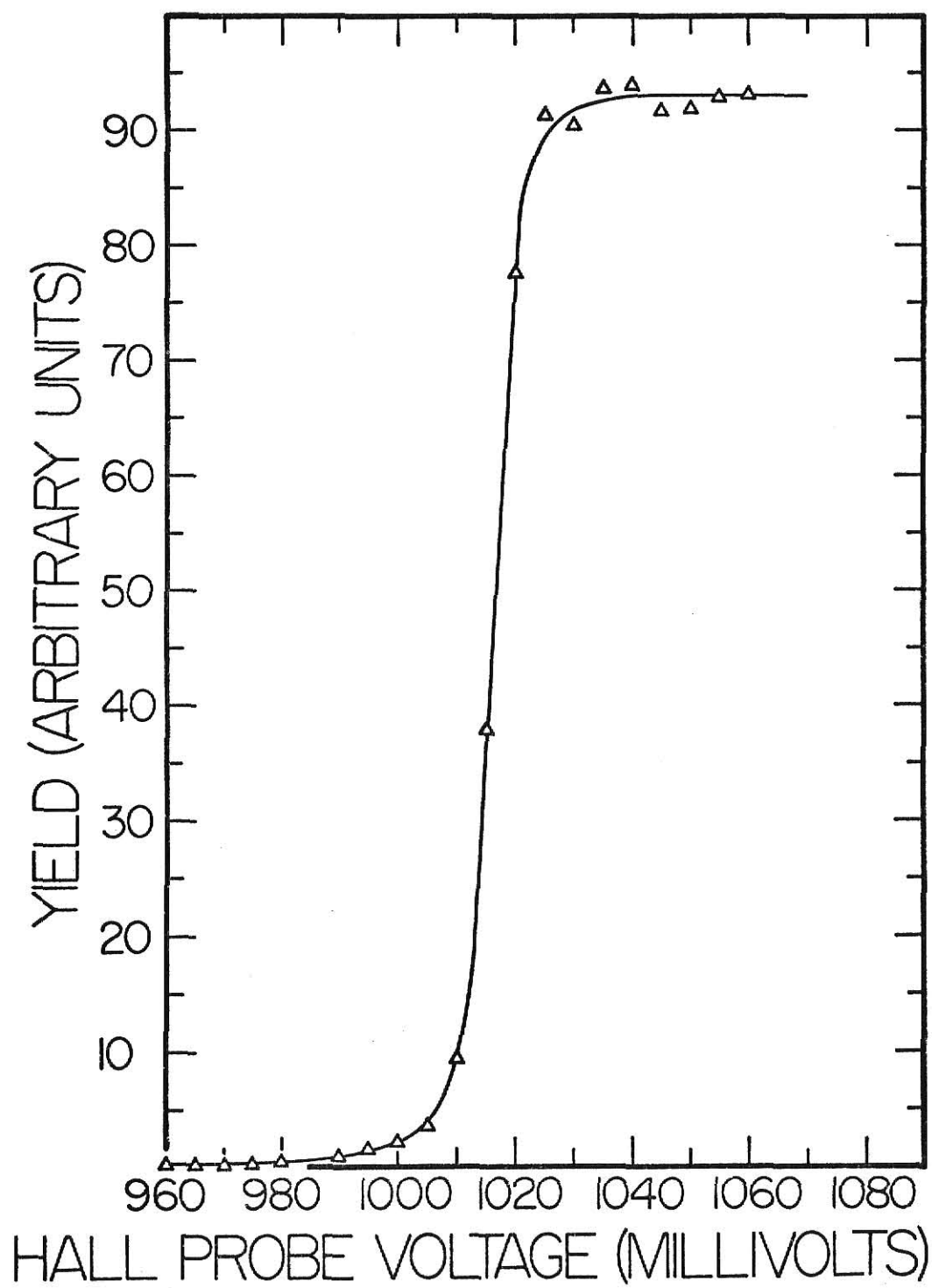


increase to a plateau and remain constant as the energy of the proton beam is increased. If the beam energy is less than 340.5 keV the compound nucleus is not excited and, thus, few gamma rays are detected. As the energy of the beam increases past 340.5 keV an increasing number of gamma rays will be detected. As the energy of the beam increases more, the protons will lose energy as they penetrate into the crystal until they again pass through the resonant energy. The yield of gamma rays thus reaches a plateau where the number of protons that react is a constant. The resonance energy is taken to be the midpoint of the rise. In figure 14 we show the yield of gamma rays verses hall probe voltage. The hall probe voltage is a measure of the current in the switching magnet. It is related to the energy of the beam by

$$E = \frac{k V^2}{I^2} , \quad (7)$$

where E is the energy of the beam, V is the hall probe voltage, I is the hall probe current, and k is the calibration constant. For this reaction, E was taken to be 340.5 keV, both V and I were measured, and k was then calculated. The value of k was found to be $769.14 \frac{\text{keV-Amps}^2}{\text{Volts}^2}$. This made it possible to dial any energy beam of protons by checking the hall probe voltage.

Figure 14: Yield of gamma rays verses hall probe voltage.



IV. Conclusions

The differential cross section for electron capture was measured as a function of the hydrogen atom scattering angle from 0° to $.07^\circ$. It was found to decrease monotonically with scattering angle. In particular, the node in the differential cross section which had been predicted by several calculations, was not observed.

Two independent measurements were made which supported this conclusion. The measured experimental resolution was $.003^\circ$ full width at half-maximum, which was almost seven times smaller than the angle where the node was predicted. It was shown that this resolution only slightly altered the angular distribution. The measurement of the differential cross section for electron capture from nitrogen by protons showed the angular distribution falling off only slightly slower than helium. Due to the fact that the total electron capture cross sections were approximately equal, it was calculated that a 20% contamination of helium with nitrogen would have been necessary to obscure the node. (Reasonable estimates gave a contamination of less than 1%)

The results of this experiment indicate that several calculations^{6,9,11,14} which predict a node in the differential cross section for protons on helium, are inadequate. Not all calculations however, predict this node. An example is the CBK calculation by Belkic and Salin¹⁵ for protons on argon. This calculation gives fair results for the wide angle scattering ($>.04^\circ$) but underestimates the differential cross section for the small angle scattering ($<.04^\circ$).

The half angle at half maximum of the differential cross section for electron capture was measured as a function of energy. The angle decreases with energy from 20-300 keV and approaches a constant from 300-1000 keV. Although the Brinkman-Kramers calculation has some difficulties with the wide-angle scattering, it gives the best fit to this data, suggesting that its predictions for small-angle scattering may be more meaningful.

Whereas many calculations fit the proton on helium data in some scattering region, no calculation as of this date has been totally successful.

REFERENCES

1. R. A. Mapleton, Theory of Charge Exchange (Wiley-Interscience, New York, 1972).
2. J. R. Oppenheimer, Phys. Rev. 31, 349 (1928).
3. H. C. Brinkman and H. A. Kramers, Proc. Acad. Sci. Amsterdam, 33, 973 (1930).
4. J. D. Jackson and H. Schiff, Phys. Rev. 89, 359 (1953).
5. A. M. Halpern and J. Law, Phys. Rev. A 12, 1776 (1975).
6. K. Omidvar, J. E. Golden, J. H. McGuire, and L. Weaver, Phys. Rev. A 13, 500 (1976).
7. D. R. Bates, Proc. Roy. Soc., Ser. A 247, 294 (1958).
8. T. G. Winter and C. C. Lin, Phys. Rev. A 10, 2141 (1974).
9. J. H. McGuire, private communication.
10. C. L. Cocke, J. R. Macdonald, B. Curnutte, S. L. Varghese, and R. Randall, Phys. Rev. Letters 36, 782 (1976).
11. Y. Band, private communication.
12. A. B. Wittkower and H. B. Gilbody, Proc. Phys. Soc., 90, 343 (1967).
13. C. F. Barnett and H. K. Reynolds, Phys. Rev. 109, 355, (1958).
14. A. M. Halpern, Phys. Rev., (to be published).
15. Dz. Belkic and A. Salin, J. Phys. B 9, L397 (1976).
16. R. Randall, calculations completed in program written for Ph.D. dissertation.

```

      $J08      ,TIME=(,59),PAGES=15
1      DIMENSION QX(25),QY(25),PX(25),PY(25),RX(25),RY(25),A(25,4)
2      PI=3.14159265
3      READ (5,1006) N
4      WRITE (6,1019) N
5      DO 501 I=1,N
6 501   READ (5,1009) QX(I),QY(I)
7       DO 502 I=1,N
8       PX(I)=(QX(I)+QY(I))*7071
9 502   PY(I)=(QY(I)-QX(I))*7071
10      DO 505 I=1,N
11 505   READ (5,1009) QX(I),QY(I)
12      DO 507 I=1,N
13 507   READ (5,1009) RX(I),RY(I)
14      WRITE (6,1020)
15      DO 520 I=1,N
16 520   WRITE (6,1021) PX(I),PY(I),QX(I),QY(I),RX(I),RY(I)
17      READ (5,1006) M1
18      WRITE (6,1022) M1
19      DO 509 I=1,M1
20 509   READ (5,1010) A(I,1),A(I,2),A(I,3),A(I,4)
21      WRITE (6,1023)
22      DO 510 I=1,M1
23 510   WRITE (6,1024) A(I,1),A(I,2),A(I,3),A(I,4)
24      READ (5,1009) TP,DTP
25      WRITE (6,1030) TP,DTP
26      SF=N*N*N
27      DO 600 I=1,40
28      FTP=0.0
29      DO 630 J=1,N
30      DO 630 K=1,N
31      DO 630 L=1,N
32      DX=QX(K)-PX(J)
33      IF (DX.EQ.0.0) SX=0.0
34      IF (DX.EQ.0.0) TX=0.0
35      IF (DX.EQ.0.0) GO TO 604
36      PQM=2699./DX
37      PQB=2699.-PQM*QX(K)
38      SX=(2836.-PQB)/PQM
39      TX=(6211.-PQB)/PQM
40 604   DY=QY(K)-PY(J)
41      IF (DY.EQ.0.0) SY=0.0
42      IF (DY.EQ.0.0) TY=0.0
43      IF (DY.EQ.0.0) GO TO 605
44      PQM=2699./DY
45      PQB=2699.-PQM*QY(K)
46      SY=(2836.-PQB)/PQM
47      TY=(6211.-PQB)/PQM
48 605   DX=RX(L)-TX
49      DY=RY(L)-TY
50      TR=SQRT(DX*DX+DY*DY)
51      DX=RX(L)-SX
52      DY=RY(L)-SY
53      SR=SQRT(DX*DX+DY*DY+3375.*3375.)
54      T=TR/SR*130./PI
55      IF (T.LT.0.0.OR.T.GT.A(41,1)) GO TO 910
56      DO 610 M=1,M1
57      IF (T.LT.A(M,1)) FT=A(M,2)*T+A(M,3)*T+A(M,4)
58      IF (T.LT.A(M,1)) GO TO 630
59 610   CONTINUE

```



```

60 630 FTP=FTP+FT/SF
61 DO 635 M=1,M1
62 IF (TP.LT.A(M,1)) F=A(M,2)*TP+TP+A(M,3)*TP+A(M,4)
63 IF (TP.LT.A(M,1)) GO TO 636
64 635 CONTINUE
65 636 WRITE (6,1025) TP,FTP,F
66 IF (FTP.EQ.0.0) GO TO 999
67 DO 640 M=1,N
68 640 RY(M)=RY(M)+DTP*58.50
69 690 TP=TP+DTP
70 GO TO 999
71 910 WRITE (6,1050)
72 GO TO 999
73 1006 FORMAT (I3)
74 1009 FORMAT (2F25.10)
75 1010 FORMAT (4F20.8)
76 1019 FORMAT ('1',' EACH APERTURE DIVIDED INTO ',I3,' SEGMENTS',/)
77 1020 FORMAT (7X,' PX',9X,' PY',9X,' QX',9X,' QY',9X,' RX',9X,' RY')
78 1021 FORMAT (6F12.4)
79 1022 FORMAT (/, ' THE THEORETICAL DIFFERENTIAL CROSS SECTION IS',
1 ' DIVIDED INTO ',I3,' SEGMENTS',/)
80 1023 FORMAT (6X,' ANGLE',9X,' THETASO',7X,' THETA',9X,' CONST')
81 1024 FORMAT (4E15.4)
82 1025 FORMAT (' TP = ',E10.4,10X,' FTP = ',E10.4,10X,' F = ',E12.4)
83 1030 FORMAT (//, ' STARTING THETA PRIME IS',2X,F6.4,/,
1 ' DELTA THETA PRIME IS',2X,F6.4,/)
84 1050 FORMAT (' NEGATIVE THETA FOUND')
85 999 CONTINUE
86 STOP
87 END

```

SENTRY

EACH APERTURE DIVIDED INTO 4 SEGMENTS

PX	PY	CX	CY	RX	RY
0.0270	0.0000	0.0254	0.0127	0.0495	0.0343
0.0000	-0.0270	0.0254	-0.0127	0.0495	-0.0343
-0.0270	0.0000	-0.0254	-0.0127	-0.0495	-0.0343
0.0000	0.0270	-0.0254	0.0127	-0.0495	0.0343

THE THEORETICAL DIFFERENTIAL CROSS SECTION IS DIVIDED INTO 11 SEGMENTS

ANGLE	THETASQ	THETA	CONST
0.3970E-02	-0.7623E 10	0.2591E 07	0.4553E 06
0.1394E-01	0.2661E 10	-0.8341E 08	0.6229E 06
0.1775E-01	0.8031E 09	-0.2968E 08	0.2767E 06
0.2737E-01	0.2632E 09	-0.1102E 08	0.1156E 06
0.2257E-01	0.8435E 08	-0.3760E 07	0.4202E 05
0.2456E-01	0.2511E 08	-0.1118E 07	0.1244E 05
0.3109E-01	-0.6935E 07	0.4576E 06	-0.6925E 04
0.3930E-01	-0.3075E 07	0.2102E 06	-0.2961E 04
0.5186E-01	0.3826E 06	-0.5645E 05	0.2172E 04
0.7742E-01	0.2365E 06	-0.3864E 05	0.1642E 04
0.1202E 00	0.2957E 05	-0.7218E 04	0.4468E 03

STARTING THETA PRIME IS 0.0000
DELTA THETA PRIME IS 0.0020

TP = 0.0000E 00	FTP = 0.4398E 06	F = 0.4550E 06
TP = 0.2000E-02	FTP = 0.4110E 06	F = 0.4299E 06
TP = 0.4000E-02	FTP = 0.3297E 06	F = 0.3437E 06
TP = 0.6000E-02	FTP = 0.2307E 06	F = 0.2361E 06
TP = 0.8000E-02	FTP = 0.1475E 06	F = 0.1493E 06
TP = 0.1000E-01	FTP = 0.8433E 05	F = 0.8480E 05
TP = 0.1200E-01	FTP = 0.4183E 05	F = 0.4106E 05
TP = 0.1400E-01	FTP = 0.1995E 05	F = 0.1899E 05
TP = 0.1600E-01	FTP = 0.7801E 04	F = 0.7414E 04
TP = 0.1800E-01	FTP = 0.2630E 04	F = 0.2517E 04
TP = 0.2000E-01	FTP = 0.6065E 03	F = 0.4800E 03
TP = 0.2200E-01	FTP = 0.4771E 02	F = -0.6543E 01
TP = 0.2400E-01	FTP = 0.8497E 02	F = 0.7136E 02
TP = 0.2600E-01	FTP = 0.2825E 03	F = 0.2845E 03
TP = 0.2800E-01	FTP = 0.4475E 03	F = 0.4508E 03
TP = 0.3000E-01	FTP = 0.5572E 03	F = 0.5615E 03
TP = 0.3200E-01	FTP = 0.6108E 03	F = 0.6135E 03
TP = 0.3400E-01	FTP = 0.6253E 03	F = 0.6276E 03
TP = 0.3600E-01	FTP = 0.6145E 03	F = 0.6171E 03
TP = 0.3800E-01	FTP = 0.5792E 03	F = 0.5820E 03
TP = 0.4000E-01	FTP = 0.5265E 03	F = 0.5262E 03
TP = 0.4200E-01	FTP = 0.4753E 03	F = 0.4760E 03
TP = 0.4400E-01	FTP = 0.4288E 03	F = 0.4289E 03
TP = 0.4600E-01	FTP = 0.3849E 03	F = 0.3849E 03
TP = 0.4800E-01	FTP = 0.3439E 03	F = 0.3439E 03
TP = 0.5000E-01	FTP = 0.3060E 03	F = 0.3060E 03
TP = 0.5200E-01	FTP = 0.2727E 03	F = 0.2722E 03
TP = 0.5400E-01	FTP = 0.2451E 03	F = 0.2451E 03
TP = 0.5600E-01	FTP = 0.2199E 03	F = 0.2198E 03
TP = 0.5800E-01	FTP = 0.1965E 03	F = 0.1965E 03
TP = 0.6000E-01	FTP = 0.1751E 03	F = 0.1750E 03
TP = 0.6200E-01	FTP = 0.1555E 03	F = 0.1554E 03
TP = 0.6400E-01	FTP = 0.1378E 03	F = 0.1377E 03
TP = 0.6600E-01	FTP = 0.1221E 03	F = 0.1220E 03
TP = 0.6800E-01	FTP = 0.1092E 03	F = 0.1081E 03
TP = 0.7000E-01	FTP = 0.9619E 02	F = 0.9605E 02
TP = 0.7200E-01	FTP = 0.8609E 02	F = 0.8594E 02
TP = 0.7400E-01	FTP = 0.7787E 02	F = 0.7771E 02
TP = 0.7600E-01	FTP = 0.7151E 02	F = 0.7138E 02
TP = 0.7800E-01	FTP = 0.6619E 02	F = 0.6613E 02

THE DIFFERENTIAL CROSS SECTION FOR ELECTRON
CAPTURE FROM HELIUM BY 293 keV PROTONS

by

Tom R. Bratton

B. S., Nebraska Wesleyan University, 1975

AN ABSTRACT OF
A MASTER'S THESIS

submitted in partial fulfillment of the
requirements for the degree
MASTER OF SCIENCE

Department of Physics
KANSAS STATE UNIVERSITY
Manhattan, Kansas 66506

1977

ABSTRACT

A beam of 293 keV protons was passed through a thin helium gas target where hydrogen atoms were formed by the capture of electrons. The differential cross section for electron capture was measured as a function of the hydrogen atom scattering angle from 0° to $.07^{\circ}$ by scanning a surface barrier detector along a diameter of the hydrogen beam. The overall resolution of the experiment was $.003^{\circ}$ full width at half maximum. The differential cross section was found to decrease monotonically with the scattering angle. In particular, the node in the cross section which had been predicted by various calculations, was not observed.